

Superconductivity of Cu/CuO_x interface formed by shock-wave pressure

A. V. Palnichenko^{a,*}, N. S. Sidorov^a, D. V. Shakhrai^b, V. V. Avdonin^b, O. M. Vyaselev^a, S. S. Khasanov^a

^a*Institute of Solid State Physics, Russian Academy of Sciences, Chernogolovka, Moscow region, 142432, Russia*

^b*Institute of Problems of Chemical Physics, Russian Academy of Sciences, Chernogolovka, Moscow region, 142432, Russia*

Abstract

A mixture of powdered Cu and CuO has been subjected to a shock-wave pressure of ≈ 350 kbar with following quenching of the vacuum-encapsulated product to ≈ 77 K. The ac magnetic susceptibility measurements of the samples have revealed metastable superconductivity with $T_c \approx 19.5$ K, characterized by glassy dynamics of the shielding currents below T_c . Comparison of the ac susceptibility and the dc magnetization measurements infers that the superconductivity arises within the granular interfacial layer formed between metallic Cu and its oxides due to the shock-wave treatment.

Keywords: Superconductivity, Copper-copper oxide interface, Dynamic magnetic susceptibility, Superconductive glass

1. Introduction

Since the discovery of superconductivity above 30 K in lanthanum barium copper oxide [1], many similar high-critical-temperature superconductors (HTSs) have been found [2]. Superconductivity in all of these multilayered oxides is believed to originate in the planes of copper and oxygen atoms, common to these compounds [3]. Therefore, fabrication of synthetic multilayers on the basis of the copper oxide layers is promising for realization of new HTSs [4, 5]. For example, a HTS-like phenomenon was observed by means of electric conductivity measurements in the samples consisting of Cu film deposited onto natural faces of CuO single crystal under special conditions [6]. The phenomenon manifests itself as a giant step-like rise of the electric conductivity of the samples by a factor $\approx 10^5$ as the temperature decreases below the critical value, T_c , which varied in the range 200–500 K depending on the thermal treatment conditions of the samples. At $T < T_c$, the electric conductivity of the Cu/CuO samples was found to be suppressed by applying the external magnetic field, as well as by increasing of electric current in the sample. These experimental facts suggest the superconductivity in the Cu/CuO interface with T_c significantly higher than room temperature [6].

A strong indication to superconductivity at 20–90 K has been revealed by dynamic magnetic susceptibility measurements in Cu/CuO_x samples prepared by surface oxidation of powdered copper followed by thermal treatment in vacuum [7]. By comparative dynamic and static magnetic susceptibility measurements, the superconductivity was attributed to weakly coupled superconducting islands formed spontaneously in the Cu/CuO_x interfacial areas during the heat treatment process.

Superconducting interfaces of such prepared Cu/CuO_x samples are instable at room temperature, as inferred from a decay

of the superconducting transition after a ~ 20 -hour exposure of the vacuum-encapsulated samples to room temperature. However, quenching of the vacuum-encapsulated Cu/CuO_x samples to low temperature (77 K) has helped to stabilize the superconducting Cu/CuO_x interfaces and prevent the decay of superconductivity [7].

A success in stabilization of the superconducting Cu/CuO_x interfaces by the low temperature quenching has motivated our attempts to apply a shock-wave pressure to the Cu/CuO mixture for their preparation. During the shock-wave impact, the stroke energy applied to the sample evokes relative displacements of local parts of the sample matter, resulting in a series of high-pressure shock-waves propagating throughout the sample within $10^{-6} - 10^{-9}$ s [8]. The energy of the shock-waves leads to local, non-equilibrium overheat of the sample's regions at the shock-wave front, followed by their rapid cooling (quenching) as the shock-wave is passed, thus fixing the sample in the metastable state. Furthermore, highly non-equilibrium conditions caused by propagation of the high-pressure shock-waves in the sample can stimulate phase transitions or mechanochemical reactions inaccessible by any equilibrium processes, i.e. static pressure-temperature mode, resulting in new materials [9, 10].

In this paper we report on metastable superconductivity at $T_c \approx 19.5$ K revealed by the ac magnetic susceptibility measurements of the powdered mixture of Cu and CuO subjected to shock-wave pressure of ≈ 350 kbar.

2. Sample preparation and measurement techniques

The samples were prepared by means of flat-type shock-wave pressure setup described in detail earlier in Refs. [11, 12]. The starting samples were tablets, 9.6 mm in diameter and 0.9 mm thick, prepared by pressing of 99.99%-pure copper powder, 5–50 μ m grain size, covered by 0.2 mm layer of powdered 10–40 μ m grain size, 99.99%-pure copper oxide CuO

*Corresponding author. Tel.: +7 906 095 4402; fax: +7 496 524 9701. E-mail address: paln@issp.ac.ru (A. V. Palnichenko)

of monoclinic crystal structure (JCPDS 89-5899). For preparing the superconducting Cu/CuO_x samples, the optimum value of the shock-wave pressure, within 1 Mbar range, was found ≈ 350 kbar.

After the shock-wave pressure treatment, the conservation cell was cut open and the samples were extracted. Within 3–5 min, the extracted samples were vacuum-encapsulated to a residual pressure 1–5 Pa into 5 cm-long quartz ampoules having 0.9 mm-thick walls and 6 mm outer diameter, and stored in liquid nitrogen to prevent their degradation under normal conditions. We have to note that quenching of the bare (vacuum-unsealed) shock-wave pressure treated samples into liquid nitrogen did not result in superconductivity, apparently due to destruction of the superconducting phase by adsorbed gaseous layer on the sample surface during the sample cooling. In addition, for comparative studies, the samples of compacted powdered pure Cu as well as pure CuO and Cu₂O have been prepared separately under the same conditions as described above.

The samples were studied by measuring the dynamic magnetic susceptibility, $\chi = \chi' - i\chi''$, using a mutual inductance ac susceptometer [12, 13]. The amplitude H_{ac} of the driving field ranged from 0.22 to 12 Oe, the driving frequency ν from 300 Hz to 10 kHz, and the superimposed dc magnetic field H_{dc} up to 300 Oe. In order to prevent degradation, warming of the samples was avoided and the measurements were done without unsealing the evacuated ampoule. The ampoule was mounted on the measuring insert at $T \sim 80$ K, which was then dipped into a precooled measurement cryostat.

Static magnetization of the sealed Cu/CuO_x samples was studied by SQUID magnetometer in the temperature range 5–70 K and static magnetic fields 30–300 Oe. The ac susceptibility measurements have shown that the properties of the sample sealed in the evacuated ampoule survive ~ 15 minutes exposure to room temperature, which enables standard loading routine of the SQUID magnetometer.

Crystal structure of the samples was investigated in the temperature range 70–300 K by X-ray diffraction measurements using Oxford Diffraction Gemini R diffractometer, MoK α radiation, equipped with a cooling system that enables the measurements in the flow of cold nitrogen gas. For the diffraction measurements, the sample was extracted from the quartz ampoule in the ambience of liquid nitrogen and rapidly (within 5–10 s) mounted onto the precooled goniometer of the diffractometer.

3. Experimental results

3.1. X-ray diffraction

Diffraction pattern of the shock-wave pressure treated Cu/CuO_x sample, recorded at $T \approx 75$ K, is shown in Fig. 1. All the diffraction rings in the observed pattern are a superposition of the patterns from polycrystalline CuO ($a = 4.245$ Å, space group Fm-3m), Cu₂O ($a = 4.267$ Å, space group Pn-3m) and Cu ($a = 3.615$ Å, space group Fm-3m) crystal structures corrected by the thermal expansion factor [14]. No change has been detected in the X-ray diffraction patterns of the Cu/CuO_x samples after their exposure for ≈ 20 hours at room temperature.

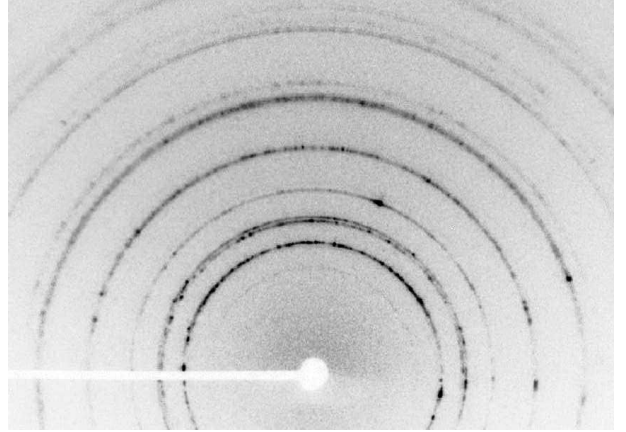


Figure 1: X-ray diffraction pattern for the shock-wave pressure treated Cu/CuO_x sample in MoK α radiation. The complete diffraction ring set is a superposition of the patterns from polycrystalline Cu, Cu₂O and CuO crystal structures.

3.2. Dynamic susceptibility

Each cycle of $\chi(T)$ measurements started from a cooldown of the Cu/CuO_x sample to 4.7 K. Next, H_{ac} was switched onto enable the measurements. Quite remarkably, at constant $T = 4.7$ K, χ' develops to the equilibrium value monotonously in time, t , towards the enlargement of diamagnetism. Curve 1 in Fig. 2a illustrates the time evolution of χ' measured at frequency $\nu = 2.1$ kHz, $H_{ac} = 0.6$ Oe and $H_{dc} = 0$. $\chi'(t)$ was found to relax exponentially to ground diamagnetic state as $a + b \exp(-t/\tau)$, shown in Fig. 2a by a solid line, where a , b and τ are fit parameters. The extracted time constant, $\tau = 7.6 \pm 1.4$ min, is practically flat in frequency for the range 0.1 - 10 kHz, as shown in Fig. 2b. We have to note that the observed $\chi'(t)$ dependencies were not influenced by an effect of the sample temperature relaxation towards the equilibrium temperature, because the $\chi'(t)$ relaxation curves were found to be insensitive to the retention interval of the sample exposure at $T = 4.7$ K ($H_{ac} = 0$) until the measurements start.

After a half-hour ($\sim 4\tau$) delay at $T = 4.7$ K ($H_{ac} = 0.6$ Oe, $H_{dc} = 0$), $\chi(T)$ dependence was measured upon heating at the rate of 1–1.5 K/min (slower heating rate made no visible change to the measurement result). The measured $\chi'(T)$ dependence is shown by Curve 1 in Fig. 2c. In this plot, the drop in $\chi'(T)$ curve at 4.7 K corresponds to the $\chi'(t)$ relaxation process, Curve 1 in Fig. 2a. As the temperature increases, a step-like rise of $\chi'(T)$ is observed at $T_c \approx 18.5$ K ($H_{ac} = 0.6$ Oe, $H_{dc} = 0$ Oe), signifying a phase transition in the sample at this temperature. In order to exclude the influence of the $\chi'(t)$ relaxation process on the $\chi(T)$ result, all subsequent $\chi(T)$ measurements were performed according to the measurement cycle described above (cooldown to 4.7 K - turn on H_{ac} , H_{dc} - half-hour delay - sweep up T and measure).

The $\chi(T)$ dependencies measured in a static magnetic field, H_{dc} , are shown in Fig. 3. According to Curves 1-3, an increase in H_{dc} suppresses the anomaly in $\chi(T)$. Increasing the driving ac magnetic field amplitude, H_{ac} , gives a similar effect, as shown in Fig. 4.

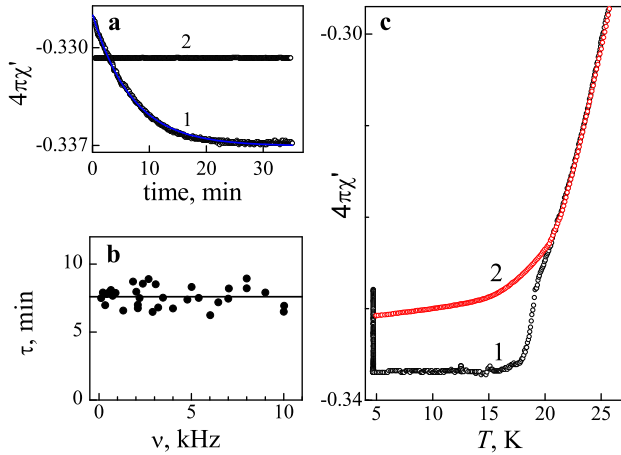


Figure 2: (a) Time evolution of $4\pi\chi'$ at $T = 4.7$ K for the vacuum-encapsulated shock-wave treated Cu/CuO_x sample (Curve 1) and for the same sample exposed to room temperature for ~ 20 hours (Curve 2). Solid curve: fit to Curve 1 in the form $a + b \exp(-t/\tau)$, where a , b and τ are fit parameters. The measurements were performed at $\nu = 2.1$ kHz, $H_{ac} = 0.6$ Oe, $H_{dc} = 0$. (b) The dependence of the time constant τ on drive frequency ν ($H_{ac} = 0.6$ Oe, $H_{dc} = 0$). (c) Temperature dependencies of $4\pi\chi'(T)$ measured before (Curve 1) and after (Curve 2) the sample exposure to room temperature ($\nu = 2.1$ kHz, $H_{ac} = 0.6$ Oe, $H_{dc} = 0$).

Fig. 5 shows the temperature dependencies of χ' and χ'' measured at frequencies from 0.3 to 10 kHz. One can see in Fig. 5 that T_c is essentially frequency independent, while the shapes of the $\chi'(T)$ and $\chi''(T)$ curves at the phase transition change dramatically with the frequency.

After completion of these measurements, the insert with the Cu/CuO_x sample was finally kept for ≈ 20 hours at room temperature. The following measurements have shown, first of all, no time dependence of $\chi'(t)$ at 4.7 K, see Curve 2 in Fig. 2a. Furthermore, the $\chi(T)$ dependence of the room-temperature-annealed sample does not exhibit a step-like anomaly and is independent on H_{ac} and H_{dc} , within the ranges used previously. Moreover, now $\chi'(T)$ and $\chi''(T)$ dependencies (Curve 2 in Fig. 2c, Curves 4 in Figs. 3, 4) are practically identical to those of pure powdered copper sample, subjected to the shock-wave pressure treatment under the same conditions. Next, $\chi(T)$ of the shock-wave pressure treated pure copper oxide (CuO , Cu_2O) samples did not reveal any anomaly in the experimental temperature range. Thus all the measuring results denote that the phase responsible for the observed anomaly in $\chi(T)$ of the Cu/CuO_x samples is related to the interfacial area, formed between the copper and copper oxide polycrystalline phases, which is unstable at room temperature.

3.3. dc magnetic moment

In contrast to the ac magnetic susceptibility, the dc magnetic moment of the shock-wave pressure treated Cu/CuO_x samples, measured using a SQUID magnetometer in a standard zero-field-cooled and field-cooling regimes, revealed no sign of the magnetic anomaly. At temperatures from 5 to 70 K, the samples demonstrated a nearly temperature-independent magnetic susceptibility ($\sim 10^{-6} \text{ cm}^3/\text{g}$) in fields $H_{dc} = 30\text{--}300$ Oe.

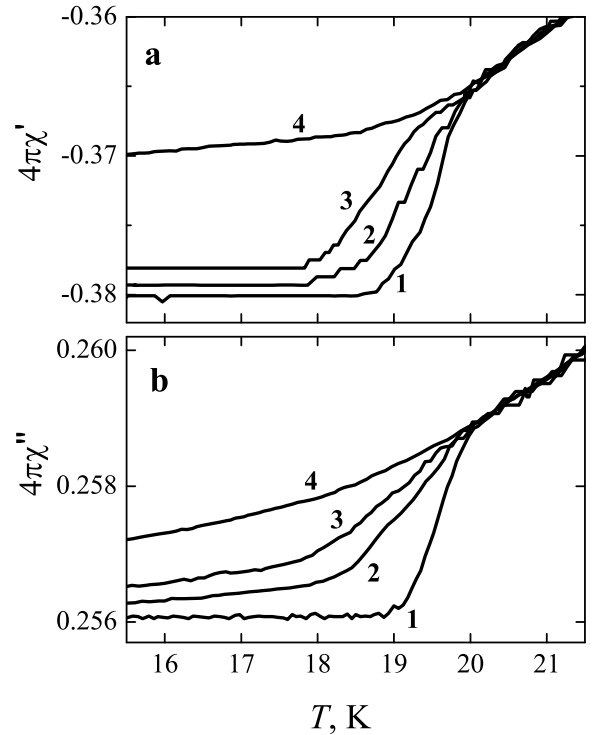


Figure 3: Temperature dependencies of the real (a) and the imaginary (b) parts of $4\pi\chi$ for the Cu/CuO_x sample measured under the dc magnetic field $H_{dc} = 0$, 168 Oe and 268 Oe (Curves 1 to 3, respectively). Curves 4 correspond to the same sample exposed for ≈ 20 hours to room temperature. The measurements were performed at $\nu = 2.94$ kHz in $H_{ac} = 0.22$ Oe.

4. Discussion

4.1. Evidence of metastable superconductivity

In the ac magnetic susceptibility measurements, the χ' response to the ac magnetic field is a function of the skin depth, $\delta \propto 1/\sqrt{\sigma\mu\nu}$, where σ and μ are, respectively, the electric conductivity and magnetic permeability of the material, and ν is the ac magnetic field frequency. According to the dc magnetic moment measurements, the Cu/CuO_x samples are nonmagnetic ($\mu \approx 1$). Moreover, no anomalies in the dc magnetic moment have been found in the range 5–70 K. Therefore, the only reason for the observed step-like anomaly in $\chi'(T)$, shown by Curve 1 in Fig. 2c, is sudden change of the electric conductivity of the sample, which we attribute to a superconducting transition.

In order to verify this assumption, the influence of magnetic field on the anomaly in $\chi(T)$ has been studied (Figs. 3, 4). The anomaly in $\chi(T)$ observed at $T_c \approx 19.5$ K for $H_{ac} = 0.22$ Oe and $H_{dc} = 0$, reduces in size and shifts to lower temperature with increasing either H_{dc} (Curves 1–3 in Fig. 3) or H_{ac} (Curves 1–3 in Fig. 4). The $\chi'(T)$ and $\chi''(T)$ dependencies presented in Figs. 3, 4 are typical for superconducting materials [15, 16] which implies a superconducting transition in the Cu/CuO_x sample.

It would be worthwhile to note that none of the constituents of the sample, neither metallic Cu nor Cu_xO ($x = 1, 2$) are superconductors in the bulk. Moreover, none of them, taken

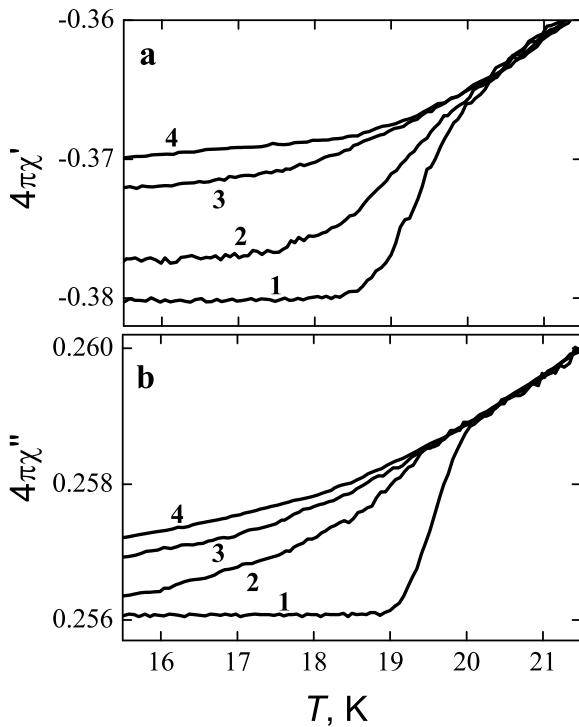


Figure 4: Temperature dependencies of the real (a) and the imaginary (b) parts of $4\pi\chi$ for the Cu/CuO_x sample measured with the amplitude of the ac driving field $H_{ac} = 0.22, 1.8$ and 11.6 Oe (Curves 1 to 3, respectively). Curves 4 correspond to the same sample exposed for ≈ 20 hours to room temperature. The measurements were performed at $\nu = 2.94$ kHz in $H_{dc} = 0$.

separately and subjected to the shock-wave pressure treatment under the same conditions, demonstrate any anomaly in $\chi(T)$. We conclude therefore that the superconductivity in the shock-wave treated Cu/CuO_x sample is related to the interfacial layer formed between copper oxide and metallic Cu phases.

One can see in Figs. 3, 4 that at temperatures well below T_c , $4\pi\chi'(T) > -1$ and $\chi''(T) > 0$, whereas a bulk superconductor assumes an ideal diamagnetic state with $4\pi\chi'(T) = -1$ and $\chi''(T) = 0$. Besides, the zero-field-cooled regime of the dc magnetization measurement has shown no sign of the superconducting transition at all. We conclude therefore that the superconducting phase formed within the interfacial layer is not a closed surface enveloping the sample, which would trap the magnetic flux and keep it constant, but rather consists of superconducting grains embedded into a non-superconducting host matrix. The grains are apparently small, less than the London penetration depth, λ , and are weakly linked by narrow, non-superconducting bridges.

In this assumption, in the dc magnetization measurements, the weak non-superconducting links result in rapid decay of the intergrain shielding current after applying the dc magnetic field, while the intragrain superconducting currents give a negligible contribution to the shielding of magnetic field due to small (sub- λ) size of the grains, thus resulting in nonmagnetic ($\mu \sim 1$) superconducting state of the sample.

On the contrary to the dc magnetization measurements, the

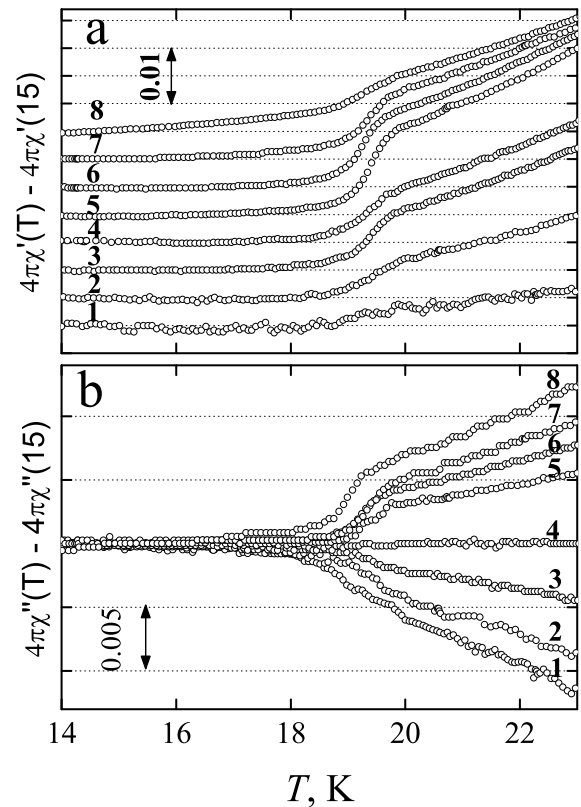


Figure 5: Temperature dependencies of the real (a) and imaginary (b) parts of $4\pi\chi$ for the Cu/CuO_x sample measured at frequencies 0.313, 0.93, 1.53, 2.1, 2.9, 3.46, 5.4 and 10.26 kHz (Curves 1 to 8, respectively). $H_{ac} = 0.22$ Oe, $H_{dc} = 0$. For visual clearness, the $4\pi\chi'(T)$ curves are separated along Y-axis by 0.005.

alternating magnetic field used in the ac magnetic susceptibility measurements maintains the intergrain shielding current. This enables the superconductivity to be detected even in discontinuous, energy dissipative loops, consisting of the weakly linked superconducting sub- λ -grains, although the diamagnetic state of such structures is quite obviously far from ideal, as observed for the Cu/CuO_x system.

As one can see in Fig. 5a, the step in $\chi'(T)$ at $T_c \approx 19.5$ K becomes bigger as the driving frequency increases from 0.313 to 2.9 kHz (Curves 1–5) and diminishes with further frequency increase (Curves 6–8). This can be explained by a superposition of normal and superconducting shielding currents, contributing to $\chi'(T)$ in the Cu/CuO_x sample.

Consider first the $\chi'(T)$ response at ≈ 19.5 K, diminishing with the frequency increase ($\nu \geq 2.9$ kHz, Curves 5–8 in Fig. 5a). This effect is well known for bulk metallic superconductors: in the normal state, increasing the ac magnetic field frequency leads to diminishing skin depth δ , hence a bigger diamagnetic signal. As a result, in the high frequency limit, the normal metal just above T_c is nearly as diamagnetic as the superconductor just below T_c which makes the superconducting transition indistinguishable in $\chi(T)$.

On the other hand, intergranular weak links in the super-

conducting Cu/CuO_x interfaces can be considered as electric capacitors connected in series into the shielding intergrain supercurrent loops. Obviously, the higher is frequency, the better the superconducting grains are linked, hence the stronger is the superconducting shielding. Apparently, this explains the growth of the $\chi'(T)$ response at $T_c \approx 19.5$ K at frequencies up to 2.9 kHz (Curves 1–5 in Fig. 5a). The two competing contributions superimpose in the studied Cu/CuO_x sample to give a maximum of the $\chi'(T)$ response to the superconducting transition at $\nu = 2.9$ kHz.

The evolution of $\chi''(T)$ with frequency is illustrated in Fig. 5b. At high frequencies (Curves 5–8), $\chi''(T)$ exhibits a step-like drop at cooling below $T_c \approx 19.5$ K, which reflects shielding of the energy-dissipative interior of the Cu/CuO_x sample by the intergrain supercurrents. The drop is vanished at low frequencies (Curves 1–4), apparently due to decreasing of the superconducting intergrain shielding at low frequencies.

As it was mentioned above, the superconducting interfaces in the Cu/CuO_x sample are unstable at room temperature (Figs. 2, 3 and 4). The reason for such instability is apparently the copper/oxygen ionic diffusion processes activated at room temperature in the Cu/CuO_x interface, which destroy the superconductivity in the sample.

The T -dependencies of χ' and χ'' measured on the degraded Cu/CuO_x samples (Curves 4 in Figs. 3, 4) are typical for normal nonmagnetic metals. Namely, as the temperature decreases, the electric conductivity of the sample increases monotonically that leads to a decrease in the skin depth δ , thus to a monotonic decrease in χ' [17]. At low temperatures, the electric conductivity becomes more flat in temperature, and $\chi'(T)$ sets constant. In turn, χ'' is also a function of δ : monotonous increase of χ'' with temperature corresponds to an increase of δ while $\delta < r$, where r is the sample depth. As the temperature continues to increase, $\chi''(T)$ reaches a maximum at T_{max} , corresponding to $\delta \approx r$, followed by $\chi''(T)$ decreasing at $\delta > r$ [17]. Therefore, an increase of the ac magnetic field frequency ν moves the T_{max} to the higher temperatures, resulting in change of the $\chi''(T)$ slope with the frequency at $T > T_c$, observed in Fig. 5b.

4.2. Superconductive glass

In granular superconductors, the superconducting grains are weakly coupled into closed loops supporting the shielding supercurrents in response to an external ac magnetic field. Due to the positional disorder of individual superconducting grains, the supercurrent loops can form multiple states of nearly equal energy. However, energy barriers between these states tend to inhibit hops from one energy state to another, resulting in time-dynamics of the frustrated shielding supercurrents similar to that observed in spin glasses [18, 19, 20].

In our experiments, the glassy behavior of the supercurrent loops in the Cu/CuO_x sample is evident from the observed slow $\chi'(t)$ relaxation into the lower energy diamagnetic ground state at 4.7 K (Fig. 2a). The relaxation time, $\tau = 7.6$ min, was found frequency independent in the range 300 Hz–10 kHz. The insensibility of τ to the excitation frequency ν is presumably a consequence of a significant time-scale mismatch between the

$\chi'(t)$ relaxation process and the ac magnetic field oscillation period, $\tau \gg 1/2\pi\nu$. This result is qualitatively similar to that for the shock-wave pressure treated Mg/MgO samples [12]. The origin of such a long $\chi'(t)$ relaxation process is rather puzzling. No clear explanation for the observed dynamics of $\chi'(t)$ in a weak ac magnetic field has been found on the basis of existing approaches that involve collective creep or vortex-glass theories for granular superconductors [20].

4.3. Nature of the Observed Superconductivity

Although the room-temperature exposure of the Cu/CuO_x samples leads to a dramatic decay of the superconducting fraction, no corresponding change has been detected in the X-ray diffraction patterns (Fig. 1). The fraction of the superconducting phase is therefore too small to be detected by the X-ray diffraction technique. In addition, none of the constituents of the sample, neither metallic Cu nor Cu_xO ($x = 1, 2$), taken separately and subjected to the shock-wave pressure treatment under the same conditions, demonstrate any anomaly in $\chi(T)$. We believe therefore that the superconductivity in the shock-wave pressure treated Cu/CuO_x samples is related to the interfacial layer formed between copper oxide and metallic copper phases.

One may reasonably ascribe the superconductivity in the Cu/CuO_x samples to some unknown superconducting copper oxide structure, unstable under the normal conditions and located at the interfacial areas in the Cu/CuO_x sample. For example, we could suppose a two-dimensional CuO lattice which is formed on the surface of CuO in the Cu/CuO interfaces. This lattice, consisting of Cu²⁺ and O¹⁻ ions, may form a narrow, partially filled two-dimensional band. In this case, the onset temperature of Bose-Einstein condensation may take a value of $T_c \sim 1000$ K [21].

However, the superconductivity has been discovered for other similar objects based on metals of various groups and their oxides (Mg/MgO [12, 22], Na/NaO_x [23], Al/Al₂O₃ [24] and Fe/FeO_x [25]). This indicates the generality of the observed phenomenon, related to the oxygen state at the interface, rather than a unique property of Cu/CuO_x system [21].

Alternatively, consider isolated nanometer-sized metallic clusters which may spontaneously arise in the granular metal-oxide interfacial areas, formed during the shock-wave pressure [12] or the surface oxidation processes [7, 22, 23, 24, 25]. Delocalized electrons of such cluster are expected to form narrow, partially filled energy band at the Fermi level, resulting in a new hypothetical family of high- T_c (> 100 K) superconductors [26, 27, 28, 29].

Besides, two-dimensional metal/oxide interfacial areas, formed in the Cu/CuO_x sample, may play a role of asymmetric confining potentials in the system of free electrons, resulting in the lack of spatial inversion symmetry at the interfaces, which may stimulate to a topological change of the Fermi surface, due to the spin-orbit splitting, and lead to the enhanced superconductivity [30].

Acknowledgement

We gratefully acknowledge useful discussions of the results with V. V. Rysanov. The work has been supported by RAS Presidium Programs "Quantum physics of condensed matter" and "Thermal physics and mechanics of extreme energy impacts and physics of strongly compressed matter" as well as RFBR grant No. 13-02-01217a.

References

References

- [1] J. G. Bednorz, K. A. Müller, Possible high T_c superconductivity in the Ba-La-Cu-O system, *Zeitschrift für Physik B Condensed Matter* 64 (1986) 189 – 193.
- [2] N. Plakida, High-Temperature Cuprate Superconductors, volume 166 of *Springer Series in Solid-State Sciences*, Springer Berlin Heidelberg, 2010. doi:10.1007/978-3-642-12633-8.
- [3] A. J. Leggett, What do we know about high T_c ?, *Nature Physics* 2 (2006) 134 – 136.
- [4] J.-M. Triscone, O. Fischer, Superlattices of high-temperature superconductors: synthetically modulated structures, critical temperatures and vortex dynamics, *Reports on Progress in Physics* 60 (1997) 1673 – 1721.
- [5] S. Gariglio, J.-M. Triscone, Oxide interface superconductivity, *Comptes Rendus Physique* 12 (2011) 591 – 599.
- [6] V. V. Osipov, I. V. Kochev, S. V. Naumov, Giant electric conductivity at the CuO-Cu interface: HTSC-like temperature variations, *Journal of Experimental and Theoretical Physics* 93 (2001) 1082 – 1090.
- [7] N. S. Sidorov, A. V. Palnichenko, S. S. Khasanov, Superconductivity in the metallic-oxidized copper interface, *Physica C: Superconductivity* 471 (2011) 247 – 249.
- [8] G. I. Kanel', V. E. Fortov, S. V. Razorenov, Shock waves in condensed-state physics, *Physics-Uspokhi* 50 (2007) 771 – 791.
- [9] V. E. Fortov, Intense shock waves and extreme states of matter, *Physics-Uspokhi* 50 (2007) 333 – 353.
- [10] N. S. Sidorov, A. V. Palnichenko, V. V. Avdonin, D. V. Shakhrai, O. G. Rybchenko, S. S. Khasanov, M. K. Sakharov, Superconductivity at 50K in a mixed-phase Ca/P/O compound system treated by shock-wave pressure up to 65GPa, *Solid State Communications* 150 (2010) 1108 – 1111.
- [11] Y. A. Ossipyan, N. S. Sidorov, A. V. Palnichenko, O. M. Vyaselev, M. V. Kartsovnik, M. Opel, V. V. Avdonin, D. V. Shakhrai, N. V. Biktimirova, A. A. Golyshev, Superconductivity of C_{60} fullerite intercalated with Ca by means of shock-wave pressure technique, *Chemical Physics Letters* 457 (2008) 74 – 77.
- [12] N. S. Sidorov, A. V. Palnichenko, D. V. Shakhrai, V. V. Avdonin, O. M. Vyaselev, S. S. Khasanov, Superconductivity of Mg/MgO interface formed by shock-wave pressure, *Physica C: Superconductivity* 488 (2013) 18 – 24.
- [13] D.-X. Chen, V. Skumryev, Calibration of low-temperature ac susceptometers with a copper cylinder standard, *Review of Scientific Instruments* 81 (2010) 025104(1) – (10).
- [14] The international centre for diffraction data JCPDS, Available at <http://www.icdd.com>, 2008.
- [15] R. A. Hein, ac magnetic susceptibility, Meissner effect, and bulk superconductivity, *Phys. Rev. B* 33 (1986) 7539 – 7549.
- [16] T. Ishida, R. B. Goldfarb, Fundamental and harmonic susceptibilities of $YBaCuO_{7-\delta}$, *Phys. Rev. B* 41 (1990) 8937 – 8948.
- [17] L. D. Landau, E. M. Lifshitz, *Electrodynamics of Continuous Media*, volume 8 of *Course of Theoretical Physics*, Pergamon, New York, 1984.
- [18] A. P. Young (Ed.), *Spin Glasses and Random Fields*, volume 12 of *Directions in Condensed Matter Physics*, World Scientific, Singapore, 1998.
- [19] C. Ebner, D. Stroud, Diamagnetic susceptibility of superconducting clusters: Spin-glass behavior, *Phys. Rev. B* 31 (1985) 165 – 171.
- [20] G. Blatter, M. V. Feigel'man, V. B. Geshkenbein, A. I. Larkin, V. M. Vinokur, Vortices in high-temperature superconductors, *Rev. Mod. Phys.* 66 (1994) 1125 – 1388.
- [21] I. I. Amelin, Possible mechanism of superconductivity in the CuO-Cu interface, *JETP Letters* 76 (2002) 185 – 188.
- [22] N. Sidorov, A. Palnichenko, O. Vyaselev, Superconductivity in Mg/MgO interface, *Physica C: Superconductivity* 480 (2012) 123 – 125.
- [23] N. S. Sidorov, A. V. Palnichenko, S. S. Khasanov, Superconductivity in the metallic/oxidized sodium interface, *Solid State Communications* 150 (2010) 1483 – 1485.
- [24] N. S. Sidorov, A. V. Palnichenko, S. S. Khasanov, Metastable superconductivity of the Al/Al₂O₃ interface, *JETP Letters* 94 (2011) 134 – 136.
- [25] N. S. Sidorov, A. V. Palnichenko, I. I. Zverkova, Superconductivity in the metallic/oxidized iron interface, *Physica C: Superconductivity* 471 (2011) 406 – 408.
- [26] J. Friedel, BCS superconductivity for weakly coupled clusters, *Journal de Physique II* 2 (1992) 959 – 970.
- [27] V. Z. Kresin, Y. N. Ovchinnikov, 'Giant' strengthening of superconducting pairing in metallic nanoclusters: large enhancement of T_c and potential for room-temperature superconductivity, *Physics-Uspokhi* 51 (2008) 427 – 435.
- [28] Y. N. Ovchinnikov, V. Z. Kresin, Cluster-based superconducting tunneling networks, *Phys. Rev. B* 85 (2012) 064518(1) – (3).
- [29] B. Cao, C. M. Neal, A. K. Starace, Y. N. Ovchinnikov, V. Z. Kresin, M. F. Jarrold, Evidence for high t_c superconducting transitions in isolated Al₄₅ and Al₄₇ nanoclusters, *Journal of Superconductivity and Novel Magnetism* 21 (2008) 163 – 166.
- [30] E. Cappelluti, C. Grimaldi, F. Marsiglio, Topological change of the fermi surface in low-density Rashba gases: Application to superconductivity, *Phys. Rev. Lett.* 98 (2007) 167002(1) – (4).